LOCOMOTION IN UNCERTAIN LOW-GRAVITY ENVIRONMENTS

*Friederike Wolff[1], Rainer Krenn[2]

[1]DLR, Münchener Straße 20, 82234 Weßling, Germany, E-mail: friederike.wolff@dlr.de

[2]DLR, Münchener Straße 20, 82234 Weßling, Germany, E-mail: rainer.krenn@dlr.de

ABSTRACT

Locomotion on asteroids is a notoriously difficult problem because small planetary bodies present a large variety of different environments that cannot adequately be defined before the mission. When internal actuators are used for object motion generation, controlling the motion requires special and computationally efficient techniques. Apart from the technical challenges, operational constraints pose tight constraints on the fine-tuning of the locomotion device to a specific environment. This paper presents the case study of the lander MASCOT (Mobile Asteroid surface SCOuT) which is a nano-lander that has been launched as a piggy-back spacecraft on JAXA's Hayabusa2 (HY2) mission.

1. INTRODUCTION

The paper will begin by presenting the MASCOT mission and provide the context in which the mobility unit inside the MASCOT lander is used. The target asteroid, the operations schedule to characterize it and the resulting requirements on the locomotion device will be shown. Subsequently, the paper details the individual parts of the optimization framework that is used to generate motions that match those requirements. The results are analyzed and the performance of the entire framework investigated.

2. MISSION BACKGROUND

In the summer of 2018, the lander MASCOT (Mobile Asteroid surface SCOuT) will arrive at the near-Earth asteroid (NEA) Ryugu, where it will be separated from the Hyabusa2 spacecraft and subsequently perform multi-point *in-situ* scientific data collection on the asteroid surface. To enable the analysis of multiple sites, the lander has been equipped with a mobility unit, an internal single-degree-of-freedom device that can impart torques and forces on the lander, thus enabling it to move.

Due to the uncertainty inherent to an exploration mission, the design of the locomotion mechanism takes place without knowledge of the requirements posed by the environment, necessitating a flexible method to adapt its behavior after the launch, thereby enabling the use of the latest mission data. This method will be presented here.

The low-gravity environment makes the dynamics of objects like landers very sensitive to even very small forces. As a consequence, a highly accurate model of the lander-ground interaction is required for the computation of robust feed-forward control parameters. It should be noted that the locomotion system of MASCOT does not receive control feedback during the motion. Only when the lander is still again, the sensors determine whether the orientation of the lander is correct. Therefore, the initial motion must be planned very tightly in order to achieve the desired result. Because the time until a moving object comes to a standstill in microgravity is so large, failure to execute a maneuver correctly leads to major delays until scientific measurements can be conducted. This is especially relevant for systems such as MASCOT that only have primary batteries.

Further constraints result from the timeline of the mission: The environment parameters cannot be determined by remote sensing from Earth and are therefore only obtained by HY2 after arrival. The release from HY2 is scheduled to be three months after arrival at the asteroid, and considering the time required for mapping, data processing and landing site selection, the maneuver generation and optimization must take place within a few weeks.

2.1. Target asteroid

The population of NEAs displays enormous variety in terms of mass, size, rotational velocity and surface characteristics. Data obtained from previous asteroid mission constitute merely a few data points on the enormous spectrum of properties.

The target asteroid of the Hayabusa2 mission is a NEA with a diameter of approximately 850 m radius. size, shape, rotation period and spin axis and are determined using an inversion of optical and thermal infrared data [1]. The quality of the method depends among other things on using data points at different angles between observer, object and Sun. Not enough good light curves could be obtained for Ryugu and as a result, a unique solution could not be found. Another restriction is that this method can only give the convex hull of the shape and will produce bad results when the object has pronounced concave parts as has been seen in the case of Churyumov-Gerasimenko. From the most likely shape model, the expected volume is computed and through combination with an estimated density, the mass. The current best estimate places the surface gravitational acceleration at 0.002 N [2].

The many assumptions that go into estimating all the individual parameters which make up the mass estimate result in almost an order of magnitude in the

variability in this essential parameter. Although Hayabusa2 will spend 1.5 years at Ryugu [2] the timeline for MASCOT is very tight. Updates will only be available once the characterization of the asteroid is completed, about one month after arrival. MASCOT will be deployed during a training approach of the surface for sample collection leaving only three weeks for the team to re-evaluate the environment model and provide new settings for the operation of the mobility.

2.2. Mobility requirements

Due to the short mission of approximately 14 hours, the lander executes all actions completely autonomously. There are three types of maneuvers to be executed:

i. **Relocation.** A relocation maneuver is performed after day and night operation of instruments at the first sampling sight and after all the date has been uplinked to Hayabusa2. The lander performs a maneuver that is designed to displace the lander by the farthest possible distance, but taking into account a constraint on the current drawn. The exact threshold for this requirement could only be defined after a prolonged test campaign that was completed half a year before the actual mission. At the same time, detailed planning of the operations on the asteroid revealed that the total time the lander takes to come to a standstill has to be less than 30 minutes. Both these cases highlight the need for a framework that is able to quickly incorporate new requirements and constraints and can rapidly re-evaluate the performance of such a mechanical system.

ii. **Uprighting.** The lander only has one correct orientation in which it can perform scientific measurements. Thus, after separation, descent, and landing, the lander has to upright in case it comes to rest on any of the other five possible sides. In this case, the GNC system determines the side facing the ground and chooses from a lookup table the correct control parameter-set for execution. Uprighting is also performed after a relocation maneuver, if required.

iii. **Relocation from wrong side (contingency case).** This motion will be executed in the case that an uprighting maneuver fails to execute correctly, even after several attempts. The assumption is that the lander is stuck and a higher energy motion to remove it from the position of location is performed.

Each of the three maneuver types have different mobility control parameter settings depending on the side of the lander facing the ground. In addition, for each maneuver type and attitude, three distinct parameter sets are defined to be tried successively. If an attempted maneuver does not succeed in changing the attitude of the lander, the next parameter setting is executed. Three meaningful ways of choosing these settings have been identified:

i. The set with the highest optimization criterion that rotates in the opposite solution to the most optimal solution. The rationale for this solution is that if the first motion has not led to movement, it might be due to obstruction by a boulder and rotation in the other direction will lead to a better outcome.

ii. Attempting a motion for less stiff but higher damping soil. This assumes that failure to move is the result of the maneuver not expending enough energy. A granular ground will naturally dissipate more energy than solid rock.

iii. As a last resort after several unsuccessful attempts to move it might be wise to actuate the mobility in the highest energy state for the longest time possible. This assumes that after many unsuccessful attempts, the lander must be severely stuck and the best guess is to excite it to the maximum to try to free it from its situation.

In total, 33 parameter sets are required and stored on the spacecraft's onboard computer.

3. MOBILITY UNIT

For environments with very low gravitational acceleration, wheeled locomotion is not a suitable choice to provide locomotion since such mechanisms require firm contact to the ground in order to propel a vehicle forward through friction.

3.1. Concept

The device presented here consists of an arm with a mass at its end and is actuated in order to generate a torque. The resulting contact forces between lander and ground are large in comparison with the gravitational force and can propel the lander to a new location. The mobility unit also allows for, albeit limited, attitude control. Since the lander is a cuboid and only one orientation permits the execution of scientific measurements, the mobility unit must be able to correct the attitude if the lander lies on the wrong side. The rationale for this kind of actuator was to be independent of the environment by having an entirely internal mechanism.

3.2. Detailed description

The mobility mechanism has been described in [4]. It consists of a wolfram mass of about 150 g mounted at a distance at about 7 cm distance of a rotational joint driven by a brushless DC motor.

The motion of the arm is defined by five parameters:

i. Start angle
ii. End angle
iii. Acceleration
iv. Deceleration
v. Maximum angular velocity

Multiple effects are at work during the motion of the actor: The acceleration of the arm produces a reaction torque on the rest of the lander around the axis about which the arm of the mobility units rotates (+Y). Additionally, the acceleration of the mass at the tip produces an oscillating torque about the two other axes the amplitude of which is a function of the instantaneous rotational velocity. This can be seen clearly in Figure 1 which shows the torque on the lander at the joint that connects it to the arm.

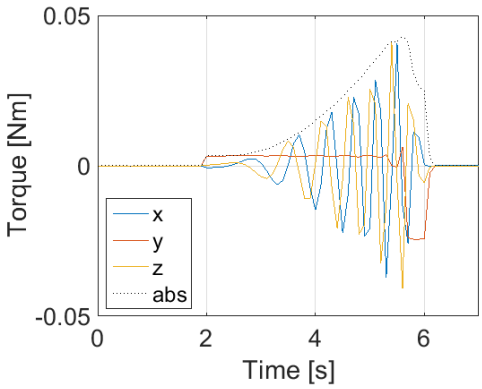

Figure 1: Torque generated at relocation operation

The maximum achievable values for acceleration and velocity are 20 rad/s^2 and 18 rad/s, respectively.

The position of the actor in the MASCOT lander is not to maximize mobility performance, but to have a high payload fraction. The 30% payload fraction in MASCOT is extremely high

, but one of the drawbacks of placing the mobility where there is space is that by being close to the center, the possible torque that can be generated about x and z is very reduced, but not negligible.

3.3. Reaction Forces and Torques

The potential to generate forces and torques that act on the lander can be approximated using the following equations:

$$T_y = \alpha \cdot m \cdot l^2$$

$$T_x = m \cdot \omega \cdot l \cdot x \cdot \cos\theta$$

$$T_z = m \cdot \omega \cdot l \cdot z \cdot \sin\theta$$

Where T is the magnitude of the torque acting upon the lander, θ, ω, α are the arm position, velocity and acceleration, m the accelerated mass, l the length of the arm and x and z the offset of the mobility position from the geometrical center. An example of the torques acting during a relocation motion is seen in Figure 1. Furthermore, the actuation produces two types of forces as a function of acceleration and rotation:

$$F_{acc} = \alpha \cdot l \cdot m$$

$$F_{vel} = m \cdot \omega^2 \cdot l$$

Using the values above, the maximum torque around the Y-axis, amounts to 0.04 Nm and oscillates, whereas for the other two axes it can be held at a constant value of 0.015 Nm.

As opposed to most methods of relocation, there is no easy way of mapping these parameters to a desired resulting motion: A genetic optimization algorithm is used to search the entire space of five-dimensional parameter sets for a solution that satisfies the specified criteria.

4. MODELLING & SIMULATION

Figure 2 shows the overview and interplay between the different parts of the optimization framework used to carry out this work. Each of the parts will be presented in the following.

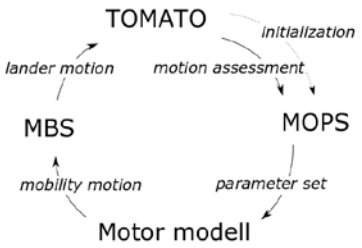

Figure 2: Interplay within the optimization framework

4.1. Mobility / Motor model

The mobility unit model is a component within the MASCOT system optimization loop that allows the optimizer to set the mobility control parameters, to compute the corresponding mobility trajectory, and to make a first assessment in terms of acceptance or rejection.

The assessment criteria are:

i. **Operation time**: The maximum operation time is limited by the onboard software to 19.95 s.

ii. **Motor current**: The motor current is limited to 2 A in order to avoid a power undersupply of the onboard computer. For short periods of less than 1 s, higher currents up to 2.5 A are also acceptable.

iii. **The relationship of velocity and acceleration control parameters:** According to the onboard software logic, the acceleration parameter has to be smaller than or equal to the velocity parameter.

If the computed mobility trajectory is compliant with these limitations, it will be accepted and applied to the MASCOT relocation or uprighting simulations. The quality of the results in terms of the optimization objectives will be subject of the second assessment.

The mobility unit model (see Figure 3) includes the following sub-models and algorithms that are present in the real mobility system as well:

i. **Onboard software:** The relevant part of the onboard software for simulation is the PI velocity control and a corresponding path planner that maps the mobility control parameters to a desired trajectory over time. The actual output of the PI velocity control is the voltage pulse width modulation (PWM) rate (0 – 100%) to be realized by the motor electronic board.

ii. **Electronic board:** The motor electronic board converts the battery voltage to lower DC values proportional to the PWM signal and provides the voltage according to the logic of a commutation table. The output of this component is the effective voltage applied to the motor.

iii. **Brushless DC Motor:** The mobility is driven by a RoboDrive ILM 25x4. In the model this motor is represented by a motor characteristic diagram based on maximum torque at zero velocity, maximum speed at zero torque and the nominal operation voltage. The output of the motor model is the input torque applied to the attached Harmonic Drive.

iv. **Harmonic Drive:** For provision of the required torque at the arm of the mobility unit, the motor torque is transmitted by a Harmonic Drive HFUC-8-2A. The dynamics of the Harmonic Drive is sufficiently represented by the velocity dependent torque losses as given in the manufacturer catalogue.

v. **Mobility unit arm:** The Harmonic Drive output torque will finally move the arm of the mobility unit. The actual arm dynamics depends on its own inertia as well as the inertia of the Harmonic Drive and the motor shaft.

The final outputs of the model are the rotational acceleration, velocity, and position of mobility unit arm over time. This is a rheonomic description of the arm trajectory that will be applied to the MASCOT multi-body model for relocation or uprighting simulations.

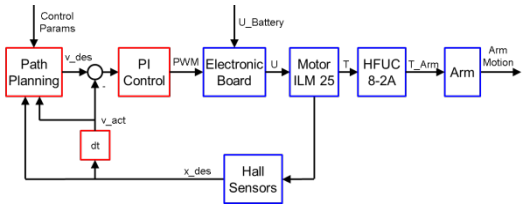

Figure 3: Block diagram of the mobility unit model

Model Parameter	Value
Battery voltage	12 V / 9 V
Max. motor torque	0.1 Nm
Max motor speed	24000 rpm
Nominal motor voltage	24 V
Gear ratio	30

Table 1: Mobility unit model parameters

The major parameters of the mobility model are concluded in Table 1. The model is validated against results of test campaigns using a copy of the MASCOT flight model. In the following diagrams (Figure 4 - Figure 6) the prediction capabilities of the mobility model regarding the aspects arm position, arm velocity, motor velocity control input (PWM signal), and motor current are presented. They show simulation results in comparison with corresponding signals recorded during test runs using MASCOT hardware. The motion control parameters applied to these experiments are documented in Table 2.

Parameter	Int. Value	SI Value
Start position of arm	0	0 rad
Stop position of arm	32000	159.57 rad
Max Velocity of arm	20	19.94 rad/s
Max acceleration of arm	9	22.43rad/s^2

Table 2: Mobility Unit Model Parameters

The diagrams in Figure 4 and Figure 5 demonstrate that the motion of the mobility unit arm (position, velocity, total duration) can be predicted very well. This capability is the primary goal of the modeling activity. The correctness of these results is crucial for the selection of suitable trajectories since the sophisticated coordination of arm position versus angular momentum change affects the relocation and uprighting performance of MASCOT significantly.

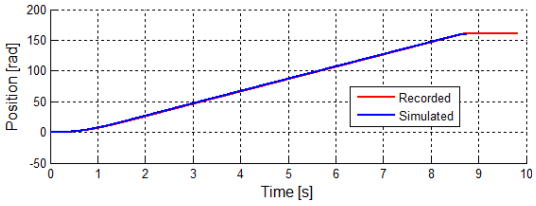

Figure 4: Prediction of the arm position

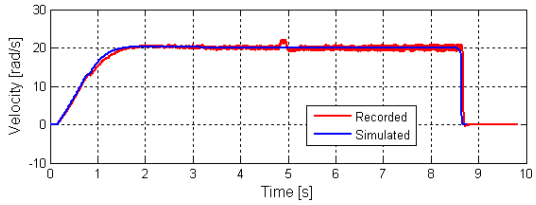

Figure 5: Prediction of the arm velocity

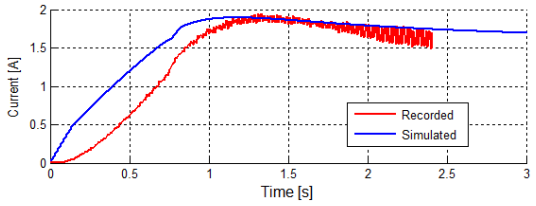

Figure 6: Prediction of the motor current

The prediction capabilities regarding motor current are not yet as good as for arm motion prediction. It seems that some minor effects of the electronic board are not

fully captured by the current model implementation. Nevertheless, the information about satisfying the current limits, which is actually needed for trajectory acceptance, is clearly visible.

4.2. Multi-body simulation

The trajectory of the arm as provided by the mobility unit model is used as an input to a multi-body simulation which is performed in SIMPACK. The Polygonal Contact Model (PCM, [5]) is used to compute the forces between the lander and the ground. The results shown in this paper have been generated with very high ground stiffness to simulate the contact with bare rock. While this is not the most likely surface of a near-Earth asteroid (NEA) such as Ryugu, if does represent a worst case in terms of the sensitivity of the motion. Because the gravity is so low, very small forces have a strong effect on the motion of the lander. If the surface is hard and penetration into the ground is almost zero, the motion becomes even more sensitive to the initial conditions and the geometry. The situation is worsened by the geometry of the object in question: The structure of the lander is not designed to facilitate the contact with ground. The corners are sharp unlike considered in other concepts [6] and the behavior of the system becomes sensitive to the point at which it is almost chaotic. The fact that solutions can still be found for all desired motions under these circumstances can therefore considered to be a strong indicator that for less stiff grounds, a solution will always be found and at a computational cost smaller than in the case presented here.

4.3. Optimization Framework

The optimization framework is called TOMATO (TOol for MAscot Trajectory Optimization) and has been presented in [6]. This paper presents the further development of this framework to make it more computationally efficient and keep up with the increasing demands of the mission design and operations.

For every motion, attitude, and set of environment parameters, an optimization has to be performed to find a set of control parameters that result in the desired motion. The Multi-Objective Parameter Optimization (MOPS) framework [8] developed by DLR is used to this end.

The previous version of TOMATO presented in [6] assumes that different physical quantities can be optimized independently of each other. Therefore, the angles, the angular velocity and the acceleration are optimized in sequence while at each stage the other parameters are held constant. The increased performance resulting from a better choice of optimization parameters has enabled optimization in the full 5D parameter space, thereby increasing the chance of finding the global optimum.

4.3.1. Relocation

The following changes contributed towards a much reduced optimization time:

i. Termination of motion immediately after the jump is initiated: the simulation was only executed until the geometric center reached a height of half the diagonal of the cuboid:

$$z > \frac{d}{2}$$

where z is the height of the geometric center of the lander above ground and d is the longest diagonal of the lander. In this way, the motion is only computed for less than 10 seconds instead of up to 40 minutes for a full relocation motion.

ii. Instead of using the achieved range by taking the position of the lander at the end of the simulation, the ballistic range was used:

$$R_{ballistic} = \frac{v^2}{g} \cdot \sin 2\theta$$

where v is the translational velocity at the start of the jump, g is the gravitational acceleration and θ is the angle between the velocity vector and the horizontal.

iii. The previous approach had the disadvantage that two settings could produce similar distances after the first parabola, but due to different orientations of the lander upon contact would bounce in different directions, at times increasing, but at other times decreasing the range. The ballistic range removes this erratic behavior and allows for more rapid convergence of the algorithm. This is illustrated in Figure 7 by the number of different parameter sets that had to be evaluated in order to converge to an optimum: Whereas the previous method required 3017 different parameter-sets, using the ballistic range this number could be reduced to only 350.

4.3.2. Uprighting

The uprighting optimization uses one criterion that is computed as follows:

$$[\sim, \text{side2soil(t)}] = \max\left\{(T(t) \cdot N) \cdot \begin{bmatrix} 0 \\ 0 \\ -1 \end{bmatrix}\right\}$$

where the rows of N are the six normal vectors of the landers faces in its initial state, T is the transformation matrix that rotates the individual normal vectors as it moves in time, and *side2soil* is an integer designating the number of the side facing downwards at a given instant.

If at any point in time during the simulation the correct side faces the ground:

$$C = \frac{\int (side2soil == correct)\ dt}{t_{end}}$$

Otherwise:

$$C = \int \widehat{n_f} \cdot (-\hat{z})\ dt$$

where $\widehat{n_f}$ is the normal vector of the face that is supposed to be facing downwards and $\hat{z}$ is the unit

vector denoting the vertical direction. This criterion captures how much the normal vector is aligned with the direction with which it is supposed to be aligned.

Reductions in the runtime of the optimization were achieved in two ways:

i. Better criteria: In the previous version of TOMATO, a binary criterion was used that indicated only whether at the end of the simulation the lander had the correct attitude or not. In addition, a criterion to minimize the total time until rest was used. These two different criteria naturally oppose each other unless the optimization is started using an existing setting that already produces the correct attitude, but is not time-optimal. Also, no gradient exists in the attitude criterion that enables the algorithm to learn which types of parameters sets are better than others. The current solution combines two criteria that are both based on evaluating the direction of the normal vectors of the faces and that captures the intuitive idea of what a human would consider to be a good type of motion.

ii. Reducing the simulation time to 300 seconds proved to capture the essence of the motion, eliminating the need for waiting until all energy is dissipated. Further optimization using the complete motion has did not increase the quality of the resulting motion in a significant manner.

4.3.3. Hardware Constraints

The logic of the onboard software limits the acceleration parameter value to be smaller or equal to the velocity parameter. This constraint cannot easily be mapped to a constraint on the tuner of the genetic algorithm because the latter accepts only absolute bounds on each parameter and no relative constraints. This is not a feature of the exact implementation but of the concept of evolution in the genetic algorithm itself: Good parameter combinations are paired and reproduced by combining the values of two existing parameter-sets together, making it impossible to from the start exclude the creation of settings that the hardware of this case study is not suitable for. To address this problem, each parameter-set is checked after being generated by the genetic algorithm and if it does not meet the criteria, the multi-body-simulation is skipped and the individual is assigned a criterion of extremely bad value, values that are typically not produced during a normal simulation process. As a result, these invalid parameter-sets that are ranked worst. Since this rank decides on the probability of transmitting information to the next generation of parameter-sets, they are highly likely to die out quickly, as can be seen in Figure 8.

Another problem is the coarseness in the settings: whereas in Figure 7 the parameters can be varied continuously, Figure 8 shows the optimization including these constraints. Whereas the angles can be varies relatively smoothly, there are only 10 distinct values for the acceleration parameter and 20-25 for the rotational velocity parameter.

Furthermore, due to onboard battery constaints the mobility has to operate on a voltage that is only about 75 % of what was initially planned in the design phase.

5. RESULTS

This section will present in detail one solution for a relocation motion to understand the dynamics that are at play and the need to compute the complete time series of the movement instead of using an analytical model. Finally, the runtimes for the different optimizations will be presented.

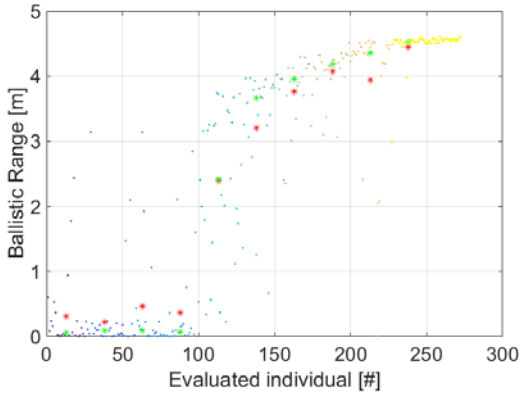

Figure 7: Successive evaluations of optimization criterion shows convergence under the assumptions of an ideal mobility

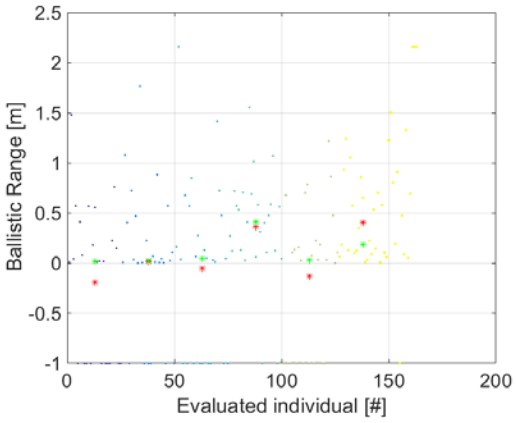

Figure 8: Successive evaluations of optimization criterion taking into account hardware limitations

5.1. Sample motion: Relocation

The highest relocation distance is achieved by using an initial arm acceleration that is not maximal. It can be seen in Figure 9 that the low initial acceleration mostly pushed the center of gravity of the lander up while the lander rotates in the direction opposite of the

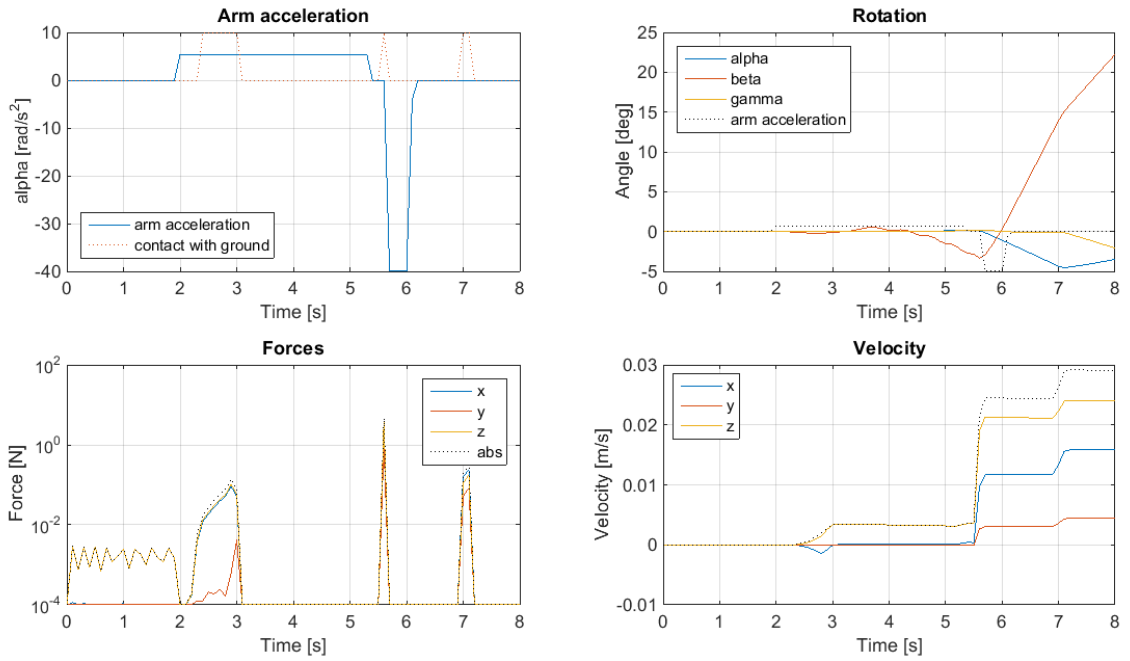

Figure 9: Sample results of a relocation operation

actor. At some point the lander loses contact with the ground, but the rotation accelerates. After the initial acceleration phase, the lander comes into contact with the ground again: the rotational kinetic energy becomes transformed into translational energy and the angular motion is reversed and increased in the opposite direction. At this point, even though no acceleration takes place, the translational velocity increases sharply, not only in z, but in x-direction.

The deceleration of the arm takes place and forces the lander into contact with the ground again. At this point, it is inclined to the surface at an angle of approximately 14° and the deceleration torque can increase the velocity parallel to the surface further.

5.2. Hardware limitations

Figure 7 shows the performance of the optimization algorithm for an ideal mobility and for the real system. It can be seen that the achieved relocation distance is reduced from ideally 11.7 m down to 2.1 m.

5.3. Performance of algorithm

Table 3 shows the runtime of the optimization runs for various maneuvers. Using the presented updates, the generation of the entire mobility catalogue could be reduced to approximately 75 h.

Overall, the optimization time was reduced by a factor of 10 compared to the initial optimization setup described in [6] even though a full polygonal model of the lander shape was used instead of a simplified substitute consisting of eight spheres applied to the corners of the lander. Differences in runtime occur due to the closeness of the initial guess by the optimization algorithm to the final optimum, but also due to the amount of time a maneuver takes to execute: whereas the initiation of relocation is a matter of seconds, changing the attitude in a controlled manner by 90° or 180° requires increasingly more time.

Movement	Runtime [h]
Upright -X	19.9
Upright -Y	6.8
Upright -Z	6
Upright +X	12.6
Upright +Y	22.8
Relocation +Z	2.1
Relocation -X	2.2
Relocation -Y	1.1
Relocation -Z	0.9
Relocation +X	0.4
Relocation +Y	0.5
Total	**75.3**

Table 3: Time to find solutions for movement

6. CONCLUSION

The paper has presented the reader with the challenges that are faced during the preparations for a mission in an almost unknown low-gravity environment.

It was shown that changes in the formulation of the optimization criteria could decrease the amount of total simulations by an order of magnitude. This highlights the need to formulate criteria that not only describe the desired output, but that are suitable for the

way that the optimization algorithm of choice operates.

As a final note, it should be kept in mind that this specific architecture of the mobility was selected in order to make the locomotion device more independent of the environment. Although contact between the moving parts and the exterior lander is avoided, it is questionable whether this system is indeed more robust than the other architectures it was initially compared to. The approach of fine-tuning a force and torque profile to initiate a very specific movement might not prove to be the best solution for motion in an unknown environment. Solutions have be found for all types of motions required for the mission, but the sensitivity to the environment and the accuracy to which the force profile must be generated might limit the practicability of the approach. The very limited ability to predict the large number of unknowns in the environment and the difficulty of verification suggest that for follow-up missions, an implementation of closed-loop control of the mobility unit with attitude sensors is strongly recommended in order to make the motion more resilient towards changes in the environment.

REFERENCES

[1] Müller, T. G., J. Ďurech, M. Ishiguro, M. Müller, T. Krühler, H. Yang, M.-J. Kim, L. O'Rourke, F. Usui, C. Kiss, B. Altieri, B. Carry, Y.-J. Choi, M. Delbo, J. P. Emery, J. Greiner, S. Hasegawa, J. L. Hora, F. Knust, D. Kuroda, D. Osip, A. Rau, A. Rivkin, P. Schady, J. Thomas-Osip, D. Trilling, S. Urakawa, E. Vilenius, P. Weissman and P. Zeidler (2017), Hayabusa-2 mission target asteroid 162173 Ryugu (1999 JU3): Searching for the object's spin-axis orientation, Astronomy and Astrophysics. A 599: A103.

[2] Wada, K., Grott, M., Michel, P., Walsh, K. J., Barucci, A.M, Biele, J., Blum, J., Ernst, C.M., Gundlach, B., Hagermann, A., Hamm, M., Le Corre, L., Lichtenheldt, R., Maturilli, A., Messenger, S., Miyamoto, H., Mottola, S., Nakamura, A.M., Müller, T., Ogawa, K., Okada, T., Palomba, E., Sakatani, N., Senshu, H., Takir, D., Zolensky, M.E., and International Regolith Science Group (IRSG) in Hayabusa2 project (2018), Asteroid Ryugu Before the Hayabusa2 Encounter, Space Science Reviews.

[3] Y. Tsuda, M. Yoshikawa, M. Abe, H. Minamino, S. Nakazawa (2013), System design of the Hayabusa2—asteroid sample return mission to Ryugu, Acta Astronautica.

[4] Reill, J., Sedlmayr, H.-J., Neugebauer, Ph., Maier, M., Krämer, E., Lichtenheldt, R., (2015) MASCOT - Asteroid Lander with Innvoative Mobility Mechanism. ASTRA - 13th ESA Symposium on Advanced Space Technologies for Robotics and Automation, 11-13 May 2015, Noordwijk, The Netherlands

[5] Hippmann, G., (2003) An Algorithm for Compliant Contact between Complexly Shaped Surfaces in Multibody Dynamics, ECCOMAS IDMEC/IST 01-04 July 2003, Lisbon, Portugal.

[6] Lichtenheldt, R., Spytek, J., Reill, J., (2015) Coaching Mascot for broad-jumping: Multi-criterial optimization of the arm trajectories for Mascot's hopping locomotion, 11th International Academy of Astronautics (IAA) Low-cost Planetary Mission Conference - LCPM-11 2015, 09-11 June 2015, Berlin.

[7] Y. Tsuda, M. Yoshikawa, M. Abe, H. Minamino, S. Nakazawa (2013), System design of the Hayabusa2—asteroid sample return mission to Ryugu, Acta Astronautica.

[8] Joos, H.-D.; Bals, J.; Looye, G.; Schnepper, K.; Varga, A.: A multi-objective optimisation-based software environment for control systems design, IEEE International Conference on Control Applications and International Symposium on Computer Aided Control Systems Design, Glasgow, Scotland, UK, pp. 7-14, 2002

[9] Jet Propulsion Laboratory, 'Hedgehog' Robots Hop, Tumble in Microgravity (Hedgehog: Online at: https://www.jpl.nasa.gov/news/news.php?feature=4712 (as of 23th April 2018)